Published as: *Nat Immunol*. 2010 March ; 11(3): 207–215.

Hematopoietic Stem Cell Differentiation Regulated by a Single Ubiquitin Ligase: Substrate Complex

Linsey Reavie[1,2], **Giusy Della Gatta**[3], **Kelly Crusio**[1,2], **Beatriz Aranda-Orgilles**[1,2], **Shannon M. Buckley**[1,2], **Benjamin Thompson**[1,2], **Eugine Lee**[1,2], **Jie Gao**[1,2], **Andrea L. Bredemeyer**[4], **Beth A. Helmink**[4], **Jiri Zavadil**[2,5], **Barry P. Sleckman**[4], **Teresa Palomero**[3], **Adolfo Ferrando**[3], and **Iannis Aifantis**[1,2]

[1] Howard Hughes Medical Institute and Department of Pathology, New York University School of Medicine, New York, NY 10016

[2] NYU Cancer Institute and Helen & Martin S. Kimmel Stem Cell Center, New York University School of Medicine, New York, NY 10016

[3] Institute for Cancer Genetics, Columbia University, New York, NY 10032

[4] Department of Pathology and Immunology, Washington University School of Medicine, St. Louis, MO 63110

[5] Center for Health Informatics and Bioinformatics, New York University School of Medicine, New York, NY 10016

Abstract

Hematopoietic stem cell (HSC) differentiation is regulated by cell-intrinsic and extrinsic cues. In addition to transcriptional regulation, post-translational regulation may also control HSC differentiation. To test this hypothesis, we visualized ubiquitin-regulated protein stability of a single transcription factor, c-Myc. The stability of c-Myc protein was instructive of HSC quiescence and c-Myc protein abundance was controlled by the ubiquitin ligase Fbw7. Fine changes in stability of c-Myc protein regulated the HSC “gene expression signature”. Using whole genome genomic approaches, we identified specific regulators of HSC function that are directly controlled by c-Myc binding, however adult HSCs and embryonic stem cells sense and interpret distinctly c-Myc regulated gene expression. These studies show a ubiquitin ligase substrate pair can orchestrate the molecular program of HSC differentiation.

Correspondence should be addressed to I.A. (iannis.aifantis@nyumc.org).
Dr. Iannis Aifantis, Howard Hughes Medical Institute, New York University School of Medicine, 550 First Avenue, MSB 504, New York, NY 10016, iannis.aifantis@nyumc.org, Phone: 212 263 5365, Fax: 212 263 8211

Author Contributions

L.R. performed most of the experiments and participated in the preparation of the manuscript. G.D.G, T.P., A.F. and B.A-O have designed and performed the ChIP[2] and ChIP experiments. K.C., E.L. and B.T. performed the ESC experiments. B.P.S, B.T., A.L.B, and B.A.H. generated and performed initial studies using the c-Myc/eGFP mice. J.Z. analyzed micro-array data. I.A. designed the study and prepared the manuscript.

Hematopoietic stem cell (HSC) self-renewal and quiescence are controlled by a highly orchestrated integration of environmental signals, most of them originating from the stem cell niche[1, 2]. Long term HSCs (LT-HSCs) reside at the top of the developmental pyramid as they possess the ability to self-renew and sustain hematopoiesis[3]. This fraction of HSCs remains largely quiescent or even dormant throughout the lifetime of an organism. Cells that receive differentiation-promoting niche signals are able to generate multi-potent progenitors (MPPs), cells that have diminished self-renewal and can enter further differentiation routes that will lead them to generate progenitors of the myeloerythroid or lymphoid lineages.

Intense experimentation during the last two decades suggested that tight control of HSC differentiation is controlled by the interplay of a handful genetic and epigenetic regulators of gene transcription[4, 5]. However, transcriptional control is unlikely to provide the complete answer to the puzzle of stem cell differentiation. It is thus intriguing to suggest that post-transcriptional or even post-translational regulation plays an essential role. The emergence of microRNA function in both embryonic and adult stem cell biology is one example[6]. Another emerging paradigm of post-translational modification is mono- or polyubiquitination of protein substrates leading to alteration of target half-life or modification of activation status. Ubiquitination is performed by large enzymatic complexes that include ubiquitin activating and conjugating components as well as adapters that dictate substrate specificity[7, 8]. One of the most important and well-characterized outcomes of protein ubiquitination is targeting to and subsequent degradation by the proteasome. By controlling protein stability and abundance, ubiquitin ligases regulate distinct biological processes, including cell cycle entry and progression[9].

Previous studies have suggested that ubiquitination, proteosomal degradation and protein stability could also control stem cell function in different organisms[10–13]. These studies introduced the intriguing hypothesis that fine-tuning of the half-life, stability and abundance of key regulators by the ubiquitin–proteasome machinery could control HSC function, specifically, self-renewal and differentiation. Testing this hypothesis *in vivo* is a challenging task as it requires quantitative assessment of substrate abundance in small stem cell and progenitor subsets. To overcome this limitation, we utilized gene-targeted mice in which relative protein abundance can be studied *in vivo* using flow cytometry and microscopy. As a model ubiquitin-substrate, we selected the transcription factor c-Myc, a well-known oncogene and developmental regulator[14, 15]. c-Myc expression and function has been suggested to be important for HSC differentiation and more specifically for HSC niche retention and survival[16, 17]. However, the molecular mechanism by which c-Myc controls HSC function is largely unknown. For example, similar amounts of *Myc* mRNA are detected in HSC and differentiated progenitors[16]. This finding introduces the hypothesis that c-Myc functions in stem and progenitor cells are more likely to be controlled post-translationally rather than at the level of transcription. Moreover, several studies have shown that c-Myc protein stability is controlled by the ubiquitin system. At least three distinct E3 ligases (Skp2, Huwe1 and Fbw7)[18–20] are involved its regulation.

We demonstrate here that relative abundance of nuclear c-Myc protein was instructive of HSC quiescence and self-renewal status, and c-Myc stability in HSC was controlled by a single E3 ubiquitin ligase, Fbw7. Deletion of *Fbw7* led to the overexpression of c-Myc

protein in single HSC cells and reduction of c-Myc abundance rescued the *Fbw7*$^{-/-}$ HSC phenotype. Moreover, we demonstrate that the HSC gene expression signature was controlled by fine changes in relative stability of c-Myc protein and identify specific gene-regulators of HSC quiescence and self-renewal. Whole genome chromatin immunoprecipitation experiments identify genes that are directly regulated by c-Myc promoter-binding and transcriptional activity. Finally, we contrast adult HSC with *in vitro* self-renewing embryonic stem cells (ESCs). We demonstrate that each stem cell type is able to sense and interpret c-Myc abundance and c-Myc-regulated gene expression in distinct ways. Our studies offer the first example of an ubiquitin ligase–substrate pair able to orchestrate the molecular program of adult mammalian stem cell differentiation.

RESULTS

c-Myc protein abundance in single HSC and progenitors

To visualize c-Myc protein abundance *in vivo,* we took advantage of a recently generated animal model[21], in which the eGFP reporter replaced the start codon of *Myc* within the second exon in the *Myc* locus, generating a functional N-terminally tagged c-Myc protein that faithfully mirrored the expression of endogenous protein. *Myc*$^{eGFP/eGFP}$ homozygous mice were viable, with no alterations in the kinetics of hematopoietic differentiation or immune function. *Myc*^{eGFP} was not expressed in lineage-positive (Lin^{+}), mature bone marrow (BM) cells, but its expression became evident when we focused on Lin^{-} progenitors (Fig. 1a–c). The highest expression of c-Myc (Myc-eGFP) was detected in the myeloerythroid progenitor fraction (MP), a cell population that originates directly from Lin^{-}, Sca-1^{+}, c-Kit^{+} (LSK) cells and is actively proliferating. To further validate the faithful expression of the c-Myc-eGFP fusion, we purified wild-type Lin^{-} c-Kit^{+} progenitors and Lin^{+} cells from whole bone marrow. Endogenous c-Myc protein was only expressed in the progenitor fraction (Fig. 1d). These experiments showed that c-Myc protein expression was detectable in the LSK fraction and peaked at the MP stage in adult bone marrow.

c-Myc protein correlates with HSC differentiation

We noticed that LSK cells, a population containing HSCs and multipotential progenitors, possessed both a c-Myc-eGFP^{+} and a c-Myc-eGFP^{-} fraction (Fig. 1e). HSCs differentiate through intermediate stages, generating at least two subsets of multipotential progenitors (MPP1 and MPP2)[22]. Only long-term (LT)-HSCs have the ability to self-renew and are largely quiescent or even dormant[22]. Therefore, we subdivided the LSK fraction using both SLAM markers (CD150 and CD48) (Fig. 1f and Supplementary Figure 1) and Flt-3 with CD34 (not shown). A substantial increase in c-Myc protein (Fig. 1f) correlated perfectly with differentiation stage as, LT-HSCs were almost (>95%) exclusively c-Myc-eGFP^{-} whereas the MPP1 fraction was the first subset with detectable c-Myc protein and further increases c-Myc protein abundance occurred in more differentiated CD150^{-}CD48^{+} MPP2 cells. To examine whether the c-Myc expression changes that we observed were independent of transcriptional control, we compared *Myc* mRNA expression in the different populations. *Myc* transcription was not elevated as LT-HSCs differentiated (Fig. 1g), suggesting that the protein changes that we identified were largely due to post-

transcriptional mechanisms. These data connect relative c-Myc protein abundance to specific stages of HSC differentiation.

Effects of extrinsic stress signals on c-Myc expression

We then sought to determine whether environmental cues, for example stress or tissue injury, could feedback on LSK proliferation and c-Myc protein abundance. Initially, we discovered that c-Myc protein abundance was not only suggestive of the differentiation stage but also dictated cell cycle status. Indeed, c-Myc-eGFP^{lo} LSK cells were exclusively in G0/G1 phases and c-Myc-eGFP^{hi} cells were actively cycling (Fig. 1h). Moreover, as tissue injury can induce exit of HSCs from quiescence, we used the chemotherapeutic agent fluorouracil (5-FU) to induce myeloablation, a process that normally activates quiescent HSCs[23]. Consistent with this notion, a 2–3 fold increase of LSK numbers from 5-FU treated *Myc*$^{eGFP/+}$ mice had entered cell cycle 2 days post treatment when compared to non-treated controls. Most importantly, these cells purified from 5-FU treated animals demonstrated substantially increased amounts of c-Myc protein (Supplementary Fig. 2). These experiments show that extrinsic stress signals can affect c-Myc protein expression in primitive hematopoietic progenitors, illustrating an intriguing feedback regulation.

c-Myc protein expression predicts self-renewal status

These observations suggested that c-Myc protein abundance (but not mRNA) could dictate the potential of HSCs to self-renew and influence their ability to differentiate. To test this hypothesis we used fluorescence activated cell sorting (FACS) to divide the LSK population into c-Myc-eGFP^{hi} and c-Myc-eGFP^{lo} cells (Fig. 2a). To achieve an estimate of the differentiation capacity of these two populations, we seeded each subset on colony forming unit (CFU) assays using cytokine-supplemented methylcellulose media. The first plating showed that the c-Myc-eGFP^{hi} fraction had an increased (two to three fold) capacity to generate colonies, however, replating of the sorted c-Myc-eGFP^{hi} expressing LSKs yielded a total inability in colony formation, reflecting a putative loss in *in vitro* self-renewing capacity. In contrast, the c-Myc-eGFP^{lo} population efficiently generated colonies after the first replating, retaining characteristics of *bona fide* self-renewing HSCs (Fig. 2b). To support these observations with *in vivo* studies, competitive reconstitutions were performed using 1000 LSK cells purified from both fractions (expressing the marker CD45.2). In agreement with the *in vitro* studies, c-Myc-eGFP^{lo} cells had the ability to efficiently compete (50:50) and generate all mature lineages as well as stem and progenitor cells 25 weeks after transplantation (Fig. 2c,d). On the other hand, c-Myc-eGFP^{hi} cells were less efficient (6–10% that of the c-Myc-eGFP^{lo} population) in generating long-term chimerism, suggesting that this population is largely devoid of LT-HSC activity (Fig. 2c,d). A previous study suggested that aging could affect differentiation ability of HSCs due to aberrant DNA repair[24]. As all the experiments described above were performed using 6–10-wk-old animals we asked whether the c-Myc-dependent regulation of HSC self-renewal is a central control mechanism in adult HSCs independently of HSC age. We repeated these experiments using aged (>60-wk-old) HSC. As shown in Supplemental Figure 3a, old and young HSCs demonstrate identical c-Myc-eGFP profiles. Colony assays and bone marrow transplantation assays further proved that relative abundance of c-Myc protein dictate LSK long-term reconstitution ability (Supplementary Figure 3b and data not shown). These findings support

the notion that the abundance of c-Myc protein expression can predict the HSC stage and that upon c-Myc protein stabilization HSC cells lose their ability to self-renew.

Fbw7 regulates c-Myc protein abundance in adult HSC

These observations suggested that c-Myc-regulated adult HSC self-renewal could be controlled by a post-transcriptional and likely a post-translational mechanism of regulation. To start probing this hypothesis, we studied the expression pattern of three enzymes, members of the ubiquitin-proteasome system (UPS) that have been previously suggested as putative regulators of c-Myc protein stability (Huwe1, Skp2, Fbw7)[25]. One of these genes, *Fbw7*, demonstrated a reciprocal expression pattern when compared to c-Myc-eGFP protein expression (Fig. 1g). To further examine whether Fbw7 controls c-Myc protein stability in HSCs, we generated Mx1-Cre^{+}*Fbw7*$^{\text{flox/flox}}$*Myc*$^{\text{eGFP/eGFP}}$ mice. Mx1 is an type I interferon (IFN)-inducible promoter[26] that is activated by intra-peritoneal injection of polyI-polyC resulting in inducible expression of Cre-recombinase and subsequent deletion of the *Fbw7* locus. We reasoned that if c-Myc is a *bona fide* substrate of Fbw7 in HSCs then deletion should significantly stabilize the c-Myc protein, an effect that will correspond to an elevated eGFP mean fluorescence intensity. Consistent with this hypothesis, c-Myc-eGFP abundance in polyI-polyC injected Mx1-Cre^{+}*Fbw7*$^{\text{flox/flox}}$*Myc*$^{\text{eGFP/eGFP}}$ LSK cells was substantially higher than their control, polyI-polyC injected Mx1-Cre^{+}*Fbw7*$^{+/+}$*Myc*$^{\text{eGFP/eGFP}}$ counterparts (Fig. 3a). More importantly, c-Myc protein was more stable in the LT-HSC compartment as defined by the SLAM markers CD150 and CD48 upon deletion of *Fbw7*. (Fig. 3b). Such stabilization was also evident in both the MP subset and in thymic CD4^{-}CD8^{-} double negative (DN) T cell progenitors. Moreover, there were no significant differences on the abundance of *Myc* mRNA expression between the different genotypes (not shown). Thus, these data provide *in vivo* support of the interaction between c-Myc protein stability and Fbw7 enzymatic function in HSCs.

Reduction of c-Myc rescues Fbw7$^{-/-}$ HSC phenotypes

To further prove the relevance of c-Myc stabilization in *Fbw7*$^{-/-}$ LSK cells, we attempted to rescue the Fbw7 deficiency-induced HSC phenotype by decreasing the c-Myc protein expression[14]. As total c-Myc deficiency completely abrogates HSC differentiation[16], [17] (Fig. 3e), we generated *Fbw7*$^{-/-}$ LSK cells that lack a single copy of c-Myc (Mx1-Cre^{+}*Fbw7*$^{\text{flox/flox}}$*Myc*$^{\text{flox/+}}$). Deletion of a single *Myc* allele rescued LSK numbers, cell cycle status and *in vitro* self-renewal capacity (Fig. 3c–e). The combined data illustrated in Fig. 2 and Fig. 3 suggest that c-Myc protein stability in HSCs is largely controlled by the activity of the Fbw7 ligase. These results are consistent with our studies that were unable to detect stabilization of additional Fbw7 substrates (Notch1/3, c-jun, cyclin E) in *Fbw7*$^{-/-}$ hematopoietic progenitors (data not shown and [12]).

Fbw7–c-Myc interplay controls LT-HSC differentiation

The previous observations led us to predict that *Fbw7* deletion should decrease LT-HSC absolute cell numbers and, conversely, *Myc* deletion should – at least phenotypically – expand the HSC subset. To test this hypothesis, we initially induced *Fbw7* deletion using the Mx1-Cre model (Mx1-Cre^{+}*Fbw7*$^{\text{flox/flox}}$ mice). Deletion of *Fbw7* rapidly led to a significant

decrease in LSK frequency (Supplemental Fig. 4a). Likewise, within the LSK subset, there was an obvious decline in the frequency and total cell number of $CD150^{+}$ $CD48^{-}$ LT-HSC subset (Supplemental Fig. 4b,c) suggesting that *Fbw7* deletion promotes the LT-HSC to MPP developmental transition and explaining the loss of LT-HSC activity observed in $Fbw7^{-/-}$ animals. On the other hand, inducible deletion of *Myc* lead to an opposite phenotype characterized by the accumulation of $CD150^{hi}$, $Flt3^{-}$, $CD34^{-}$ LT-HSC-like cells (Supplemental Fig. 4d–g). These results further support *in vivo* the role of the antagonistic interplay between the ubiquitin ligase (Fbw7) and substrate in the differentiation and self-renewal capacity of HSCs.

c-Myc abundance controls the molecular program of HSC

To further understand the mechanistic impact of c-Myc protein stabilization in HSCs, we purified c-Myc-$eGFP^{hi}$ and c-Myc-$eGFP^{lo}$ subsets and used whole-genome transcriptome analysis to define the gene expression signatures of each population. A substantial alteration of the gene expression program accompanies the transition from c-Myc-$eGFP^{lo}$ to c-Myc-$eGFP^{hi}$ stages (Fig. 4a). Indeed, stabilization of c-Myc protein correlated with upregulation of cell cycle (including *Ccnd1, CcnA2, Bub1, Aurka, Skp2, Cdk2*), transcription (including *Narg1, Tcerg1, Ilf3, E2F2, E2F3*) and epigenetic (including *Ezh1, Suv39h2*) regulators. Consequently, a large number of genes known to regulate HSC self-renewal (including *Evi1, Eya1, Meis1, Hoxa5/9, Hoxb3, Cdkn1c, Egr1*) were significantly down-regulated in the c-Myc–$eGFP^{hi}$ subset. Further analysis has revealed a striking overlap of gene expression signatures between c-Myc–$eGFP^{hi}$ and $Fbw7^{-/-}$ LSKs (Fig. 4a) underlining the close biological connection between the two molecules and further explaining the loss of self-renewal capacity of $Fbw7^{-/-}$ HSCs. Further studies using the Gene Set Enrichment Analysis (GSEA) tool[27] provided additional information on shared gene clusters between the c-Myc-$eGFP^{lo}$ versus c-Myc-$eGFP^{hi}$ signature and publicly available datasets. A sizable correlation exists between the c-Myc-$eGFP^{lo}$ gene signature and several published HSC-related datasets (Fig. 4b). Conversely, the c-Myc-$eGFP^{hi}$ signature was significantly enriched in datasets presenting genes that positively control cell cycle progression, DNA replication and c-Myc-induced genes in different cell types[28–30]. Similarly, KEGG pathway/DAVID database analysis showed significant enrichments associated with cell cycle, DNA replication, and metabolism in the c-Myc-$eGFP^{hi}$ population (not shown). Interestingly, further GSEA analysis revealed significant enrichment of TGF-β and Wnt–β-catenin pathway-regulated genes in the c-Myc-$eGFP^{lo}$ signature (Fig. 4c and Supplementary Fig. 5). Both pathways have been implicated in the regulation of HSC differentiation and self-renewal[31, 32]. These studies correlate the relative abundance of a single transcription factor to the gene expression signature that defines HSC quiescence and self-renewal.

Identification of genes directly controlled by c-Myc

These results are of unique significance as they suggest that c-Myc protein stability is a central regulator of gene expression programs that influence HSC self-renewal, transcription and cell cycle entry. To further explore the mechanism of c-Myc-controlled gene regulation we have compared the identified microarray signatures to our whole genome Chromatin Immunoprecipitation ($ChIP^{2}$) datasets that contain loci occupied by c-Myc factors in c-Myc-expressing leukemia (T-ALL) cells[33]. This comparison demonstrated a significant

enrichment for genes overexpressed in the c-Myc-eGFP^{hi} subset within the TALL Chip^{2} dataset (Fig. 5a). The majority of these genes also belonged to functional categories related to cell cycle progression, transcription, translation and epigenetic control (Fig. 5 and Supplemental Figure 6). To demonstrate the validity of these whole-genome wide ChIP^{2} studies we have selected ten genes previously suggested to play important roles in the regulation of cell cycle progression, gene translation and transcription. Using this model-gene subset we performed conventional ChIP. As predicted, the c-Myc binding sites on the promoters of all these genes were indeed occupied by the c-Myc factor (Fig. 5b).

As the presented database was generated using human c-Myc-expressing hematopoietic tumor (leukemia) cells we sought to further validate these studies using mouse c-Kit-expressing stem and progenitor cells. We were able to demonstrate that the genes bound by c-Myc illustrated in Fig. 5b were also transcriptionally regulated by c-Myc in BM HSCs and progenitor cells (Fig. 5b,c and Supplementary Fig. 7). These genes were expressed in wild-type HSCs, highly expressed in the c-Myc-eGFP^{hi} subset and silenced in HSCs purified from compound *Myc*$^{-/-}$ mice (*Myc* and *Mycn*)[16]. To further rule out the possibility that present findings were biased due to the ChIP database used, we selected a group of genes that are overexpressed in the c-Myc-eGFP^{hi} LSK subset and also have highly conserved (between mouse and human) putative c-Myc binding sites. We performed conventional ChIP using highly purified bone marrow Lin^{-} c-Myc-eGFP^{hi} progenitors and showed that a significant portion of these genes promoters were indeed bound by c-Myc factors (Fig. 5c). Collectively, these studies demonstrate a mechanistic correlation between c-Myc protein abundance, binding on regulatory DNA sites and transcriptional control of HSC differentiation.

Fbw7:c-Myc axis in fetal liver hematopoietic cells

We next sought to test the importance of the c-Myc stability in a stem cell population closely related to adult HSCs, namely fetal liver HSCs. Although very similar phenotypically and functionally, fetal HSCs actively expand in number in the fetal liver during embryonic days 12.5–14.5 (ref. [34]). Thus, we hypothesized that fetal HSCs would show higher amounts of c-Myc protein than their adult counterparts. Our experiments (Fig. 6) have validated this hypothesis. Initially, almost three-fold more fetal LSK cells were in cycle at any given moment, in agreement with previous findings (Fig 6b). Also, abundance of c-Myc protein (in E13.5–14.5 *Myc*$^{eGFP/+}$ embryos) was substantially higher in fetal total and CD150^{+} LSKs when compared to adult LSKs (Fig 6c–d).

Interestingly, *in vitro* CFU assays using purified c-Myc-eGFP^{hi} and c-Myc-eGFP^{lo} fetal HSCs revealed no differential ability to generate hematopoietic colonies in primary, secondary or tertiary plating assays (Fig 6e). These findings were consistent with transcriptome studies which showed very similar gene expression signatures between the c-Myc-eGFP^{hi} and c-Myc-eGFP^{lo} fetal LSK subsets, in contrast to the well defined and largely distinct signatures illustrated using their adult counterparts (Fig. 6f and Supplemental Fig. 8). However, long-term competitive reconstitution assays using the fetal liver c-Myc-eGFP^{hi} and c-Myc-eGFP^{lo} LSK subsets demonstrated that when introduced in an adult

environment c-Myc-eGFP^{hi} cells were unable to produce long-term chimerism, in agreement with the results obtained using their adult counterparts (Fig. 6e).

Dynamic regulation of Fbw7 and c-Myc in ESCs

To further probe the universality of the Fbw7–c-Myc interaction in stem cell self-renewal we turned to the study of embryonic stem cells (ESCs), a stem cell type with properties fundamentally distinct from adult and quiescent HSC. ESC are unique among stem cells as they can differentiate into all three germ layers and self-renew extensively in culture[35]. In terms of cell cycle regulation, ESCs proliferate rapidly, display a shortened G1 phase and possess a constitutively active cyclinE-CDK2. Furthermore, ESCs express low amounts of the D-type cyclins and have almost no CDK4 kinase activity[36]. It was thus tempting to suggest that Fbw7 could be dispensable for the self-renewal of ESCs. Indeed, our initial expression studies supported this notion as Fbw7 was expressed less in self-renewing ESCs and was upregulated as differentiation was induced (Fig. 7a). To further prove these qPCR studies we used a trapped ESC line, in which a LacZ reporter cassette was introduced in the Fbw7 locus disrupting expression monoallelically (Fig. 7b). Fbw7^{LacZ} expression was almost undetectable in self-renewing ESCs and was subsequently induced upon ESC differentiation (Fig. 7c). Although there were minimal changes in *Myc* transcript abundance between self-renewing and differentiating ESCs (Fig. 7a), c-Myc protein expression, on the other hand, was readily detectable in self-renewing ESCs and became down-regulated upon induction of differentiation (Fig. 7d), confirming multiple previous studies which connected c-Myc expression to ESC pluripotency[37, 38]. ChIP studies showed that c-Myc was not only expressed but was also detectable on the promoters of selected predicted gene targets (Fig. 7e).

Fbw7 is dispensable for self-renewal of ESCs

To address whether c-Myc stability could also be regulated by the UPS in ESCs, we treated self-renewing and differentiating ESCs with the proteasome inhibitor MG-132. We found that both total-and phospho-c-Myc protein accumulated in both self-renewing and differentiating culture conditions (Fig. 7d). Complimentary to this finding, we also treated *Myc*$^{eGFP/+}$ ESCs with MG-132 and observed stabilization of c-Myc–eGFP by flow cytometry as well as immunofluorescence using an antibody which detects eGFP (Fig. 8a,b). To begin assessing the role of Fbw7 in ESCs self-renewal and its regulation of c-Myc, we used siRNA-mediated gene silencing. ESC cell specific Fbw7 knockdown resulted in accumulation of c-Myc eGFP, suggesting that Fbw7 regulates c-Myc protein stability in self-renewing ESCs (Fig. 8c). Knockdown of Fbw7 was very efficient as measured by qRT-PCR expression assays (Figure 8d). We observed similar results in another mouse ESC line (W4) using shRNA directed against Fbw7 where knockdown resulted in accumulation of both total- and phospho-c-Myc protein (Figure 8e). However, there were no phenotypic changes (Fig. 8f) or changes in expression of germline markers demonstrating that ESCs retain characteristics associated with molecular (data not shown) effects of ESC self-renewal. In contrast, silencing of the pluripotency regulator *Nanog*, led to rapid cell differentiation and loss of self-renewal (Fig. 8f). To further test the dispensability of Fbw7 in ESCs – at least in this *in vitro* system – we used a transgenic ES cell line that reports for self-renewal due to the expression of GFP-driven by *Nanog* regulatory elements[39]. Fbw7

silencing was unable to affect *Nanog*–GFP expression and ES cell self-renewal in this system (Fig. 8g). Overall, these observations show that Fbw7 expression is upregulated during ESC differentiation and that Fbw7 silencing is dispensable for the *in vitro* self-renewal of ES cells. They also identify a significant molecular distinction between ESCs and quiescent adult stem cells (HSCs) (Supplemental Figure 9).

DISCUSSION

Our observations are the first to identify a specific ubiquitin ligase: substrate pair as a central regulator of stem cell differentiation. They demonstrate *in vivo* that slight changes in the stability and abundance of c-Myc protein expression could play the role of a rheostat controlling adult stem cell quiescence and self-renewal. Our work also explains the mechanism by which c-Myc carries out its function within the HSC population. It identifies, using whole-genome transcriptional analysis and ChIP[2] approaches, a constellation of genes that are directly regulated by relative abundance of this transcription factor during these early stages of hematopoiesis. Most importantly, our studies suggest a differential need for c-Myc stability between adult and embryonic stem cells suggesting that different stem cell types sense and interpret c-Myc-regulated gene expression in distinct ways. All these studies prove the hypothesis that the ubiquitin–proteasome system can control stem cell differentiation by directly controlling important regulators of cell cycle entry, self-renewal and/or lineage commitment. Further studies are needed to define the extent of the involvement of the ubiquotome in different aspects of stem and progenitor cell biology.

Our findings explain the discrepancy between *Myc* mRNA expression and function that has been previously demonstrated. Indeed, c-Myc deletion studies suggested that c-Myc expression is essential for the exit of HSCs from the osteoblastic niche through regulating the expression of essential adhesion molecules, including N-Cadherin[17]. However, the same investigators have shown that *Myc* mRNA stability remains stable from the LT-HSC stage to the common myeloid progenitor (CMP) stage questioning the HSC-specific function of this transcription factor[16]. These findings were verified by our own independent analysis. We demonstrate here that Fbw7 expression is high in the LT-HSC stage and virtually undetectable at subsequent MPP and MP stages of differentiation. Similarly, c-Myc protein abundance increased as HSCs differentiated and reached their peak at the MP and CMP stages. These observations explain the previously reported discrepancy and underline the importance of ubiquitin-mediated protein stability in these early stages of hematopoiesis.

One of the most exciting aspects of this study is the differential dependence of embryonic (ESC) and adult HSCs on c-Myc stability and Fbw7 activity. Indeed, adult HSCs are characterized by high Fbw7 expression and a rapid c-Myc turnover while self-renewing ESC demonstrate only a basal Fbw7 activity and a very stable c-Myc protein. Few such factors that have distinct functions in the two stem cell types have been identified thus far, most of them members of the machinery that initiates cell cycle, including cyclins D and E, cell cycle inhibitors (CDKI) and the retinoblastoma protein (pRb). It is very likely that the differential Fbw7 expression is tightly linked to the cell cycle entry machinery. Indeed, studies in embryonic fibroblasts reveal that Fbw7 expression is cell cycle-dependent, with the highest levels recorded at the G0/G1 stages (B.A-O and I.A., unpublished). The Fbw7

behavior during ES cell differentiation is consistent with c-Myc availability and its essential role in the regulation of pluripotency, however at this point we cannot exclude a role for additional ESC Fbw7 substrates that could control cell cycle progression, including cyclin E. Finally, as c-Myc was recently proved to be one of the factors controlling adult cell reprogramming[38], it is intriguing to propose that the ubiquitin system and more specifically Fbw7 could be a key regulator of this process. Our data also fit perfectly with other studies that showed that the kinase GSK3β, which phosporylates c-Myc on Thr^{58} and triggers Fbw7-mediated degradation in other cell systems[40], is largely excluded from the nucleus in self-renewing ESCs. GSK3β enters the nucleus upon ESC differentiation due to the absence of LIF-induced Akt activation[41]. We demonstrate here that both proteasome inhibition and Fbw7 knockdown leads to stabilization and overexpression of c-Myc phosphorylated on Thr^{58} connecting ESC differentiation, kinase activation, SCF^{Fbw7} complex recruitment and c-Myc degradation.

Our work also suggests that the ubiquitin complex is a novel regulator of stem cell differentiation and function. Indeed, activity of ubiquitin ligases (like Fbw7) or opposing deubiquitinases (DUB) could control both the abundance and the activation of central stem cell regulators. This close connection appears to be conserved between species as a recent report has demonstrated the requirement for the DUB *Scrawny* in the epigenetic control of gene expression in *Drosophila* stem cells[10]. These observations propose an additional layer of stem cell regulation and also suggest that genetic or chemical targeting of specific ubiquitin enzyme activity could affect somatic cell reprogramming, adult stem cell expansion and putatively cancer stem cell differentiation and oncogenicity.

METHODS

Animals

The Myc^{flox} [42] mice were a kind gift from F. Alt (Harvard University). All mice were housed in a pathogen-free animal facility at New York University School of Medicine. All animal procedures were carried in compliance with Institutional Animal Care and Use Committee of the New York University School of Medicine.

Genotyping and *in vivo* animal studies

Tails were clipped from mice 1–2 weeks after birth and incubated in tail-lysis buffer containing Proteinase-K for 24 h at 55 °C. NaCl was added and cellular debris pelleted by ultra-centrifugation. DNA was precipitated upon addition of isoproanol, pelleted and washed using 70% ethanol. DNA pellet was dissolved in water and used for PCR analysis. Primers were designed to amplify both WT and floxed *Myc* and *Fbw7* alleles. Furthermore, primers were designed to detect both WT and *Myc-eGFP* knockin alleles (Supplemental Table 2). Mice received 5 i.p. polyI:polyC injections of 20ug/gram of body weight 2 weeks after birth and analyzed 2 weeks post injection. Deletion of targeted alleles and transcript levels were measured by genomic PCR and qRT-PCR.

Quantitative real-time PCR

RNA was isolated using RNeasy-Plus Mini Kit (Qiagen). cDNA synthesis was carried out by using Super-Script III First Strand Synthesis System Reverse Transription Kit (Invitrogen) and used for qRT-PCR with iQ SYBR green supermix on an iCycler (BioRad). Relative expression was determined from cycle-threshold (C_t) and normalized to internal control, *Actb*. For primer sequences, see Supplemental table 2.

Flow cytometry and antibodies

Flow cytometric analysis was carried out as previously described [12]. In experiments utilizing the *Myc-eGFP* knock in mouse we analyzed a fluorescence minus one (FMO) littermate control in parallel to set eGFP gates (Supplementary Fig. 9). Antibodies used for FACS analysis were procured from e-Bioscience. Ki-67 antibody used for cell cycle analysis was bought from BD Biosciences. Specifically, the antibodies we used were as follows: c-kit (2B8), Sca-1 (D7), CD150 (TC-15-12F2.2), CD48 (HM48-1), Mac-1 (M1/70), Gr-1 (RB6-8C5), NK1.1 (PK136), TER-119, CD3 (145-2C11), CD19 (1D3), IL7R (RAM34), CD4 (RM4–5), CD4 (H129.19), CD8 (53 – 6.7), CD25 (PC61), and CD44 (IM7). BM lineage antibody cocktail includes: Mac-1, Gr-1, NK1.1, TER-119, CD3, IL7R and CD19.

Immunoblotting

Immunoblotting was done as previously described[12]. Briefly, c-Kit$^+$ and c-Kit$^-$ bone marrow cells were isolated using a magnetic-bead based positive selection kit with a biotynylated c-Kit primary antibody (EasySep Positive Biotin Selection kit; Stem Cell Technologies). Upon selection, cells were lysed using RIPA lysis buffer, incubated at 0 °C for 20 min, and cellular debris was pelleted using ultra-centrifugation. Total cell lysates were separated on a 4–20% Tris-HCl gradient gel by SDS-PAGE electrophoresis and transferred to nitrocellulose membrane. Membrane was probed with the following antibodies: c-Myc (SC-764; Santa Cruz Biotechnology) and tubulin (Santa Cruz Biotechnology).

Immunofluorescence

Experiments were carried out as previously described[43]. c-Kit$^+$ bone marrow cells were purified as described above (immunoblotting). Cells were aliquoted onto charged glass slides, fixed using 4% para-formalydehyde, cell membrane permeablized by 0.1% Triton-X, and incubated with GFP-specific rabbit polyclonal antibodies at 4 °C overnight (ab290; Abcam). Subsequently, washed slides were incubated with anti-Rabbit IgG alexa-488 conjugated secondary antibody (Invitrogen) and counterstained with Dapi nuclear stain (Sigma).

Gene Set Enrichment Analysis

GSEA was performed on normalized expression data as described[44]. Gene expression profiles of c-Myc-eGFP^{lo} versus c-Myc-eGFP^{hi} cell populations were used as background dataset and two different gene sets were used as foreground: “C2 curated gene sets” from the Broad Institute (http://www.broad.mit.edu/gsea/msigdb/index.jsp) and a homemade gene set

constructed by considering c-Myc Chip on chip data, *P*-value < 0.005 (ref. [33]). The differentially expressed genes are ranked using "signal to noise" metric.

Microarray Analysis

Five nanograms (5 ng) of total RNA from target cell populations was amplified and labeled using the Ovation Amplification v2 and Biotin cDNA Biotin systems (Nugen, Inc.). The resulting cDNA was hybridizated to GeneChip MG 430 2.0 arrays following recommendations of the array manufacturer (Affymetrix). The raw data were processed in GeneSpring 7.2 (Agilent). The Affymetrix CEL files were normalized using Robust Multi-Array Average expression measure (RMA) and baseline scaling[44]. To identify differentially abundant mRNAs between replicate experimental conditions, the abundance levels had to be identified as significantly different by at least one of three statistical algorithms available from TIGR Microarray Suite TM4: T-test ($P < 0.05$, α correction), Significance Analysis of Micro-array (SAM, false discovery rate set 5% and Pavlidis Template Matching (PTM, $P < 0.05$)[45]. KEGG pathway and DAVID tools were accessed through http://david.abcc.ncifcrf.gov/ for pathway enrichment analyses. The c-Myc-eGFP gene expression datasets are available through the Gene Expression Omnibus (GEO) repository (GSE19502).

Chromatin Immunoprecipitation Assay

Chip[2] and ChIP assays were performed as previously described[33] using T-ALL cell lines, $Lin^{-}c\text{-}Kit^{+}$ selected bone marrow cells and mouse embryonic stem cells (W4, 129/sj). Briefly, qRT-PCR was completed on chromatin immunoprecipitates and corresponding whole cell extracts to validate c-Myc promoter occupancy of 10 "hand-picked" genes using an ABI 7300 Real-Time PCR system (Applied Biosystems). β-actin was used as input reference.

In vitro colony forming assays

Total LSK from control, $Fbw7^{-/-}Myc^{+/-}$ $MxCre^{+}$ and $Fbw7^{-/-}Myc^{-/-}$ $MxCre^{+}$ mice or upper 30% c-Myc-$eGFP^{+/-}$ and lower 30% of c-Myc-$eGFP^{+/-}$ LSK cells were sorted from $Myc^{eGFP/eGFP}$ knock-in adult mice or E14.5 embryos. 300 cells per subset were seeded in duplicate and cultured in cytokine supplemented methylcellulose medium (MethoCult 3434; Stem Cell Technologies). Subsequently, colonies were counted on day 7, isolated, re-plated and cultured for another 7 days (total 14 days).

ES cell culture, lenitviral transduction and siRNA transfection

All embryonic stem cell lines were maintained on MEFs cultured on gelatin-coated plates in the presence of DMEM (Cellgro) supplemented with 15% FBS. The Fbw7 ESC LacZ trapped line was obtained by the Texas Institute for Genomic Medicine. $Myc^{eGFP/-}$ ESCs and *Nanog-GFP* ESCs were reverse transfected by mixing 30 nM siRNA (commercially available, siGENOME SMARTpool, Dharmacon) with Lipofectamine 2000 (Invitrogen) in supplemented DMEM media (Cellgro). siRNA mix was added to a gelatin coated 96-well plate, and ES cells were plated at 1,500 cells/well in DMEM and LIF (Chemicon). For differentiation experiments, ESC cells were pre-plated for 1 h (to remove MEFs), seeded at low density, and at 24 h post initial plating (Day 0) either only LIF was removed or LIF was

removed and Retinoic Acid was added. eGFP fluorescence was measured using an LSRII (BD Biosciences) 48 h post-transfection. *Nanog-GFP* ESC cells (kind gift from I. Lemischka) were transduced by pLKO.1-PIG lentiviruses (a gift from Ihor Lemischka see reference [35] and Supplementary Table 3) containing respective shRNAs 1 h after preplating. Two days post-transduction, transduced cells were selected by puromycin (2 μg/ml) and subsequently used for self-renewal and differentiation experiments.

Bone marrow transplantation

Freshly dissected femur and tibia were flushed using a 1cc insulin syringe filled with PBS supplemented with 3% FBS. Cells were spun for 2.5 min at 200g and red blood cells lysed using ACK lysis buffer for 3 min. at 25 °C. The cells were then washed in PBS/3%FBS and spun. Subsequently, the cells were passed through a cell strainer, counted, and stained using antibodies directed against lineage markers (PE), c-Kit (APC), and Sca-1 (Pe-Cy7). Finally, bone marrow derived CD45.2^{+} c-Myc-eGFP^{Hi} or c-Myc-eGFP^{Lo} LSK subsets (from adult mice and E14 fetal livers) were FACS purified and 1000 cells from each subset were mixed with 1.0×10^{6} wild-type CD45.1^{+} bone marrow cells and injected into the ocular cavity of lethally irradiated (2x 600rad) CD45.1 host mice. Chimerism was analyzed by peripheral blood analysis at 7,12, 17 and 25 weeks post transplantation. Chimerism in bone marrow, thymus and spleen was measured at 17 weeks.

5-FU treatment

Experiments using 5-FU were performed as previously described[16]. Briefly, *Myc*$^{eGFP/-}$ mice were injected one time with 75 μg/gram of body weight of fluorouracil and LSK population within the bone marrow was analyzed 2 days post treatment using flow cytometry.

Statistical analysis

All the statistical analyses were performed using un-paired two-tailed Student's *t*-test assuming experimental samples of equal variance, unless otherwise specified.

Supplementary Material

Refer to Web version on PubMed Central for supplementary material.

Acknowledgments

We would like to thank the members of the Aifantis Lab and specifically B. King for advice as well as time and effort spent towards this manuscript. P. Lopez and the NYU Flow Facility for expert cell sorting. The NYU Cancer Institute Genomics Facility for help with micro-array processing. M.Gostissa and F. Alt for the c-Myc^{flox} mice. I. Lemishka and his lab for the Nanog-GFP line and valuable technical advice. Supported by the National Institutes of Health (RO1CA133379, RO1CA105129, R21CA141399, R56AI070310, P30CA016087 to I.A., RO1AI41428, RO1AI072039 to B.P.S. and R01CA120196 to A.F.), the American Cancer Society (RSG0806801 to I.A.), the Mallinckrodt Jr. Foundation, the Irma T. Hirschl Trust and the Alex's Lemonade Stand Foundation (to I.A.). B.A-O. was supported by the Alexander von Humboldt Foundation. S.M.B. was supported by the NYU Hematology/Oncology Program and K.C. by the NYU Molecular Oncology and Immunology Training Grant (5T32CA009161). I.A and A.F. are Leukemia & Lymphoma Society Scholars. I.A. is a Howard Hughes Medical Institute Early Career Scientist.

References

1. Adams GB, Scadden DT. The hematopoietic stem cell in its place. Nat Immunol. 2006; 7:333–337. [PubMed: 16550195]
2. Kiel MJ, Morrison SJ. Uncertainty in the niches that maintain haematopoietic stem cells. Nat Rev Immunol. 2008; 8:290–301. [PubMed: 18323850]
3. Kondo M, et al. Biology of hematopoietic stem cells and progenitors: implications for clinical application. Annu Rev Immunol. 2003; 21:759–806. [PubMed: 12615892]
4. Yoshida T, et al. The role of the chromatin remodeler Mi-2beta in hematopoietic stem cell self-renewal and multilineage differentiation. Genes Dev. 2008; 22:1174–1189. [PubMed: 18451107]
5. Moore KA, Lemischka IR. Stem cells and their niches. Science. 2006; 311:1880–1885. [PubMed: 16574858]
6. Gangaraju VK, Lin H. MicroRNAs: key regulators of stem cells. Nat Rev Mol Cell Biol. 2009; 10:116–125. [PubMed: 19165214]
7. Cardozo T, Pagano M. The SCF ubiquitin ligase: insights into a molecular machine. Nat Rev Mol Cell Biol. 2004; 5:739–751. [PubMed: 15340381]
8. Harper JW, Schulman BA. Structural complexity in ubiquitin recognition. Cell. 2006; 124:1133–1136. [PubMed: 16564007]
9. Yamasaki L, Pagano M. Cell cycle, proteolysis and cancer. Curr Opin Cell Biol. 2004; 16:623–628. [PubMed: 15530772]
10. Buszczak M, Paterno S, Spradling AC. Drosophila stem cells share a common requirement for the histone H2B ubiquitin protease scrawny. Science. 2009; 323:248–251. [PubMed: 19039105]
11. Matsuoka S, et al. Fbxw7 acts as a critical fail-safe against premature loss of hematopoietic stem cells and development of T-ALL. Genes Dev. 2008
12. Thompson BJ, et al. Control of hematopoietic stem cell quiescence by the E3 ubiquitin ligase Fbw7. J Exp Med. 2008
13. Whetton AD, et al. The time is right: proteome biology of stem cells. Cell Stem Cell. 2008; 2:215–217. [PubMed: 18383624]
14. Dalla-Favera R, Martinotti S, Gallo RC, Erikson J, Croce CM. Translocation and rearrangements of the c-myc oncogene locus in human undifferentiated B-cell lymphomas. Science. 1983; 219:963–967. [PubMed: 6401867]
15. O'Neil J, Look AT. Mechanisms of transcription factor deregulation in lymphoid cell transformation. Oncogene. 2007; 26:6838–6849. [PubMed: 17934490]
16. Laurenti E, et al. Hematopoietic stem cell function and survival depend on c-Myc and N-Myc activity. Cell Stem Cell. 2008; 3:611–624. [PubMed: 19041778]
17. Wilson A, et al. c-Myc controls the balance between hematopoietic stem cell self-renewal and differentiation. Genes Dev. 2004; 18:2747–2763. [PubMed: 15545632]
18. Zhao X, et al. The HECT-domain ubiquitin ligase Huwe1 controls neural differentiation and proliferation by destabilizing the N-Myc oncoprotein. Nat Cell Biol. 2008; 10:643–653. [PubMed: 18488021]
19. von der Lehr N, et al. The F-box protein Skp2 participates in c-Myc proteosomal degradation and acts as a cofactor for c-Myc-regulated transcription. Mol Cell. 2003; 11:1189–1200. [PubMed: 12769844]
20. Welcker M, et al. The Fbw7 tumor suppressor regulates glycogen synthase kinase 3 phosphorylation-dependent c-Myc protein degradation. Proc Natl Acad Sci U S A. 2004; 101:9085–9090. [PubMed: 15150404]
21. Huang CY, Bredemeyer AL, Walker LM, Bassing CH, Sleckman BP. Dynamic regulation of c-Myc proto-oncogene expression during lymphocyte development revealed by a GFP-c-Myc knock-in mouse. Eur J Immunol. 2008; 38:342–349. [PubMed: 18196519]
22. Wilson A, et al. Hematopoietic stem cells reversibly switch from dormancy to self-renewal during homeostasis and repair. Cell. 2008; 135:1118–1129. [PubMed: 19062086]
23. Arai F, et al. Tie2/angiopoietin-1 signaling regulates hematopoietic stem cell quiescence in the bone marrow niche. Cell. 2004; 118:149–161. [PubMed: 15260986]

24. Rossi DJ, et al. Deficiencies in DNA damage repair limit the function of haematopoietic stem cells with age. Nature. 2007; 447:725–729. [PubMed: 17554309]
25. Eilers M, Eisenman RN. Myc's broad reach. Genes Dev. 2008; 22:2755–2766. [PubMed: 18923074]
26. Kuhn R, Schwenk F, Aguet M, Rajewsky K. Inducible gene targeting in mice. Science. 1995; 269:1427–1429. [PubMed: 7660125]
27. Subramanian A, et al. Gene set enrichment analysis: a knowledge-based approach for interpreting genome-wide expression profiles. Proc Natl Acad Sci U S A. 2005; 102:15545–15550. [PubMed: 16199517]
28. Georgantas RW 3rd, et al. Microarray and serial analysis of gene expression analyses identify known and novel transcripts overexpressed in hematopoietic stem cells. Cancer Res. 2004; 64:4434–4441. [PubMed: 15231652]
29. Ivanova NB, et al. A stem cell molecular signature. Science. 2002; 298:601–604. [PubMed: 12228721]
30. Goldrath AW, Luckey CJ, Park R, Benoist C, Mathis D. The molecular program induced in T cells undergoing homeostatic proliferation. Proc Natl Acad Sci U S A. 2004; 101:16885–16890. [PubMed: 15548615]
31. Reya T, et al. A role for Wnt signalling in self-renewal of haematopoietic stem cells. Nature. 2003; 423:409–414. [PubMed: 12717450]
32. Karlsson S. Is TGF-beta a stemness regulator? Blood. 2009; 113:1208. [PubMed: 19196870]
33. Margolin AA, et al. ChIP-on-chip significance analysis reveals large-scale binding and regulation by human transcription factor oncogenes. Proc Natl Acad Sci U S A. 2009; 106:244–249. [PubMed: 19118200]
34. Morrison SJ, Hemmati HD, Wandycz AM, Weissman IL. The purification and characterization of fetal liver hematopoietic stem cells. Proc Natl Acad Sci U S A. 1995; 92:10302–10306. [PubMed: 7479772]
35. Ivanova N, et al. Dissecting self-renewal in stem cells with RNA interference. Nature. 2006; 442:533–538. [PubMed: 16767105]
36. Orford KW, Scadden DT. Deconstructing stem cell self-renewal: genetic insights into cell-cycle regulation. Nat Rev Genet. 2008; 9:115–128. [PubMed: 18202695]
37. Silva J, et al. Nanog is the gateway to the pluripotent ground state. Cell. 2009; 138:722–737. [PubMed: 19703398]
38. Takahashi K, et al. Induction of pluripotent stem cells from adult human fibroblasts by defined factors. Cell. 2007; 131:861–872. [PubMed: 18035408]
39. Schaniel C, et al. Delivery of short hairpin RNAs--triggers of gene silencing--into mouse embryonic stem cells. Nat Methods. 2006; 3:397–400. [PubMed: 16628211]
40. Welcker M, Clurman BE. FBW7 ubiquitin ligase: a tumour suppressor at the crossroads of cell division, growth and differentiation. Nat Rev Cancer. 2008; 8:83–93. [PubMed: 18094723]
41. Bechard M, Dalton S. Subcellular localization of glycogen synthase kinase 3beta controls embryonic stem cell self-renewal. Mol Cell Biol. 2009; 29:2092–2104. [PubMed: 19223464]
42. de Alboran IM, et al. Analysis of C-MYC function in normal cells via conditional gene-targeted mutation. Immunity. 2001; 14:45–55. [PubMed: 11163229]
43. Demuth T, et al. MAP-ing glioma invasion: mitogen-activated protein kinase kinase 3 and p38 drive glioma invasion and progression and predict patient survival. Mol Cancer Ther. 2007; 6:1212–1222. [PubMed: 17406030]
44. Bolstad BM, Irizarry RA, Astrand M, Speed TP. A comparison of normalization methods for high density oligonucleotide array data based on variance and bias. Bioinformatics. 2003; 19:185–193. [PubMed: 12538238]
45. Saeed AI, et al. TM4: a free, open-source system for microarray data management and analysis. Biotechniques. 2003; 34:374–378. [PubMed: 12613259]

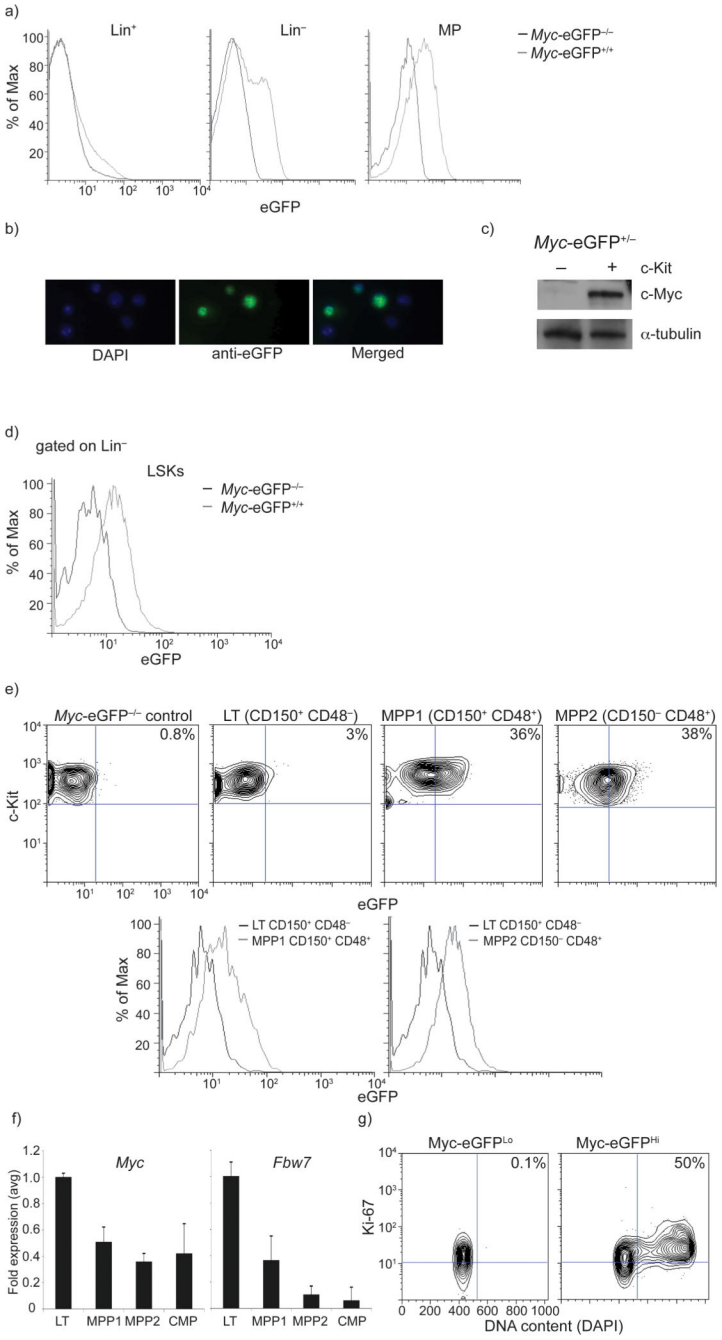

Figure 1. Visualization of c-Myc protein abundance in early hematopoiesis

a) Levels of c-Myc-eGFP expression during early hematopoiesis in Lineage$^+$, Lineage$^-$, LSK (Lineage$^-$, c-Kit$^+$, Sca1$^+$) and MP (lineage$^-$, c-Kit$^+$, Sca1$^)$ BM subsets. n=6 mice **b)** Immuno-fluorescence tracing of nuclear c-Myc-eGFP expression in Lineage$^-$ bone marrow progenitors. **c)** Western blot demonstrating presence of c-Myc protein in c-Kit$^+$ and absence in c-Kit$^-$ subset of adult bone marrow. **d)** Overlay histogram depicting c-Myc-eGFP protein expression within LSK cells. **e)** c-Myc-eGFP expression in eGFP$^{-/-}$control, LT-HSC and MPP (1, 2) populations. **f)** qRT-PCR quantification of *Myc* and *Fbw7* mRNA expression

during HSC differentiation. **g)** Levels of c-Myc-eGFP protein correlate with the cell cycle status of LSK cells. Sorted c-Myc-eGFP^{Hi} or c-Myc-eGFP^{Lo} LSK cells were analyzed using Ki-67 and DAPI staining. Plots are a representation of at least 3 independent experiments.

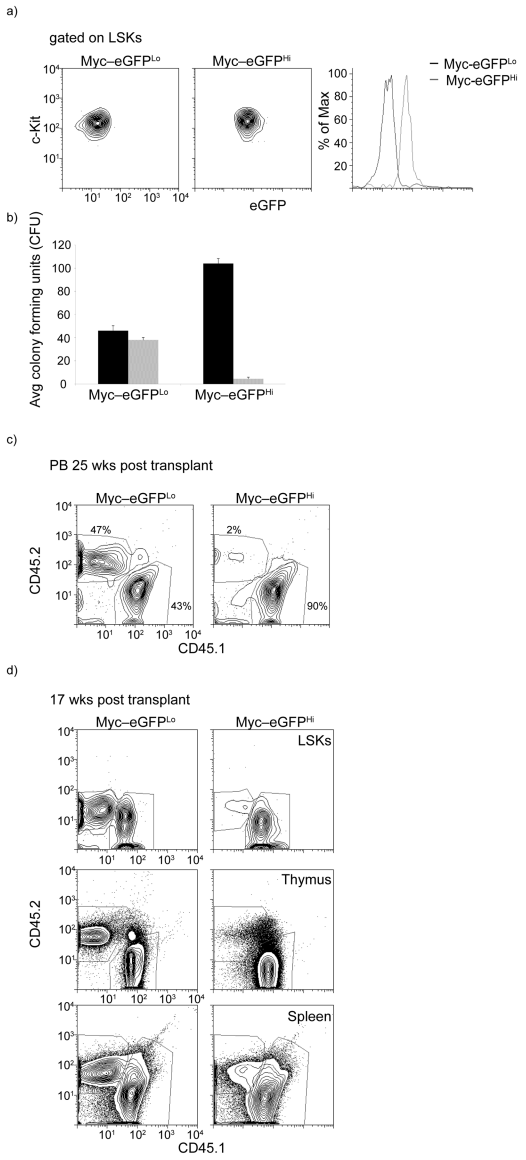

Figure 2. c-Myc protein levels correlate with loss of HSC self-renewal

a) FACS-dependent separation of c-Myc-eGFP^{Hi} and c-Myc-eGFP^{Lo} LSK populations. **b)** CFU *in vitro* cultures using sorted c-Myc-eGFP^{Hi} and c-Myc-eGFP^{Lo} cells. In black: First plating of LSKs, in grey: second plating. Error bars indicate standard deviation (Std) (n=3 mice in 3 independent experiments). **c)** Peripheral blood chimerism in competitive reconstitution assays at 25 weeks post transplant (n=3 mice). **d)** Relative chimerism of sorted c-Myc-eGFP^{Hi} and c-Myc-eGFP^{Lo} LSKs (CD45.2) in the bone marrow (LSK subset), thymus and spleen **(d)** 17 weeks post transplantation (n=3 mice).

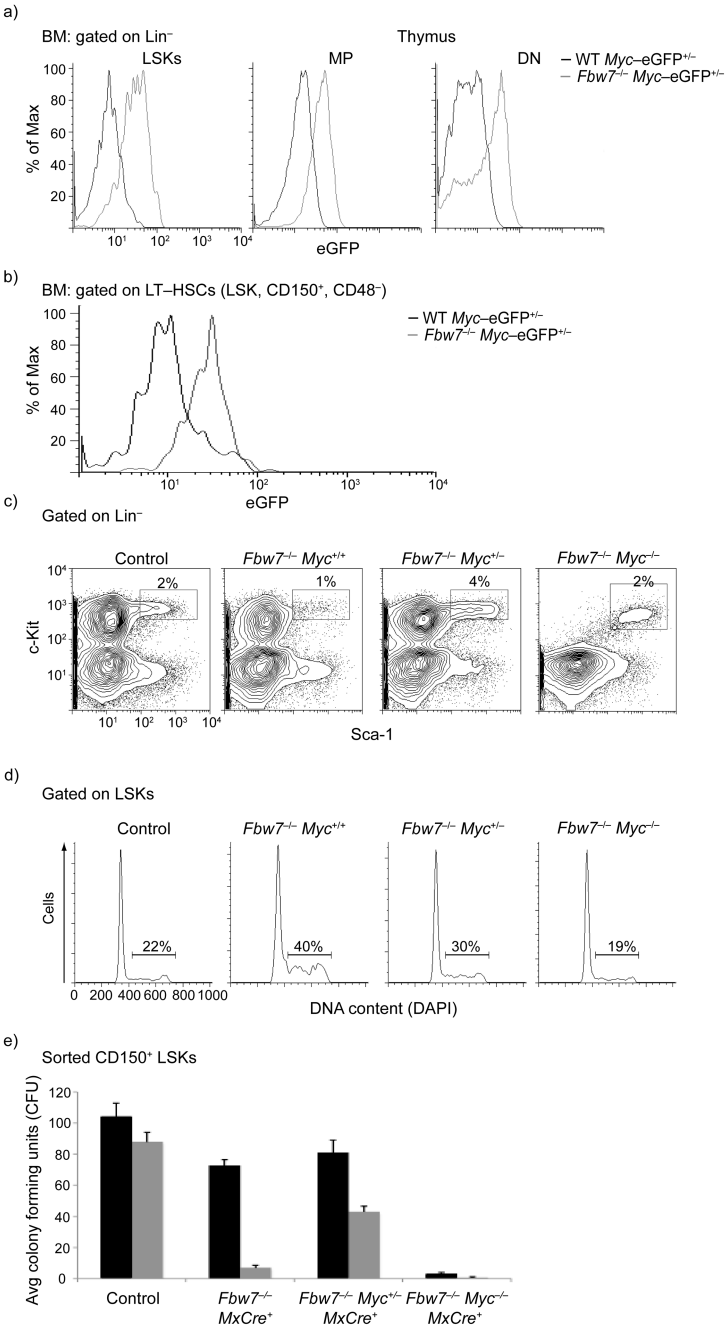

Figure 3. c-Myc protein stability in HSC is controlled by the ubiquitin ligase Fbw7

a) FACS analysis showing detection of c-Myc-eGFP in different progenitor populations. LSK, MP and thymic DN ($CD4^{-}8^{-}$) subsets are shown. **b)** FACS analysis showing stabilization of c-Myc-eGFP protein in LT-HSC subset (LSK, $CD150^{+}$, $CD48^{-}$) upon *Fbw7* deletion **c-d)** Deletion of a single *Myc* allele significantly rescues the *Fbw7*$^{-/-}$ HSC phenotype. FACS profiles of bone marrow LSKs **(c)**, cell cycle status of LSKs **(d)** and methylcellulose assays ($CD150^{+}$ LSKs) **(e)** are shown. Black: first plating, Grey: second

plating. Error bars indicate standard deviation (Std) (n=5 mice). Plots are a representation of at least 3 independent experiments.

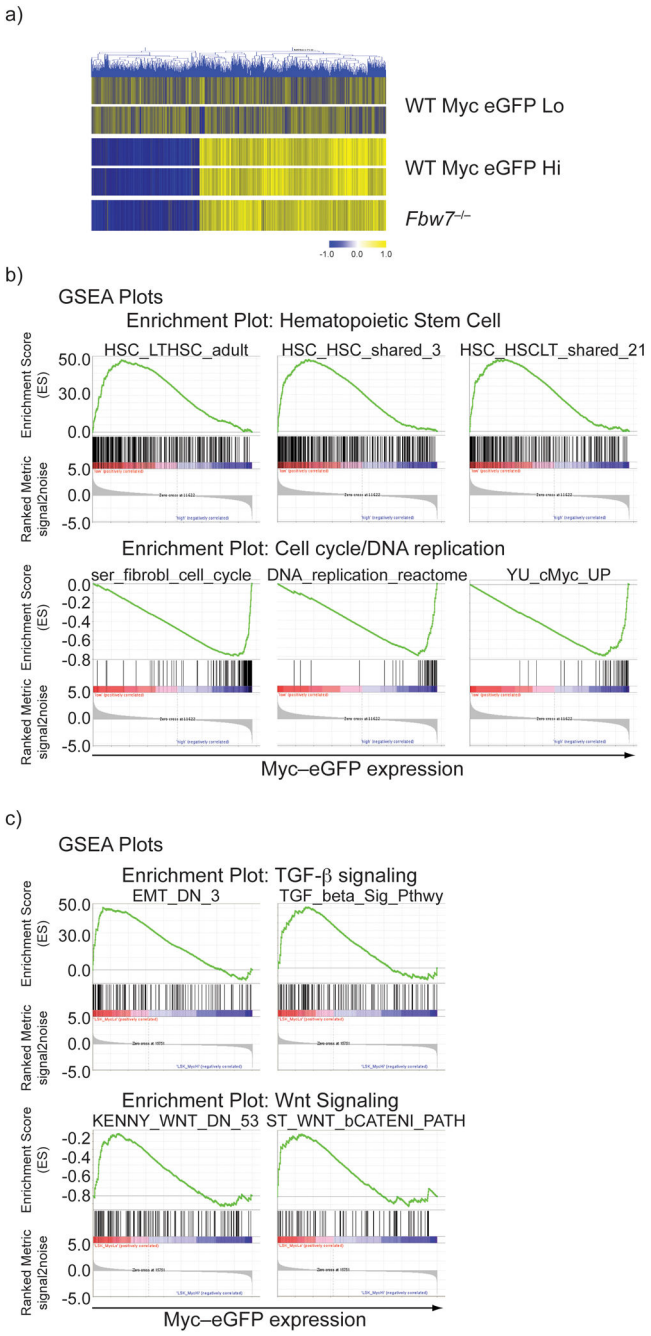

Figure 4. The role of the c-Myc:Fbw7 interaction in fetal liver stem and progenitor cells

a) FACS staining defining LSK cells in e.d.14.5 fetal liver and adult (6wk old) bone marrow. **b)** Cell cycle status of fetal and adult LSK cells. **c)** Levels of c-Myc-eGFP protein expression in fetal and adult LSK cells. The overlay histogram shows induction of c-Myc protein expression in fetal LSKs. **d)** Levels of c-Myc-eGFP protein expression in $CD150^{+}$ LSKs. **e)** Methylcellulose culture using the indicated cell populations purified from the fetal liver (fetal) or the bone marrow (adult). Black: first plating, Grey: second plating. Error bars indicate standard deviation (Std) (n= 6 mice). **f)** c-Myc-$eGFP^{Lo}$ but not c-Myc-$eGFP^{Hi}$

expressing fetal liver LSK subsets show chimerism in the peripheral blood 20wks post transplant in competitive reconstitution assays. CD45.2^{+} cells are donor-derived cells in the peripheral blood (n= 6 mice). Plots are a representation of at least 3 independent experiments.

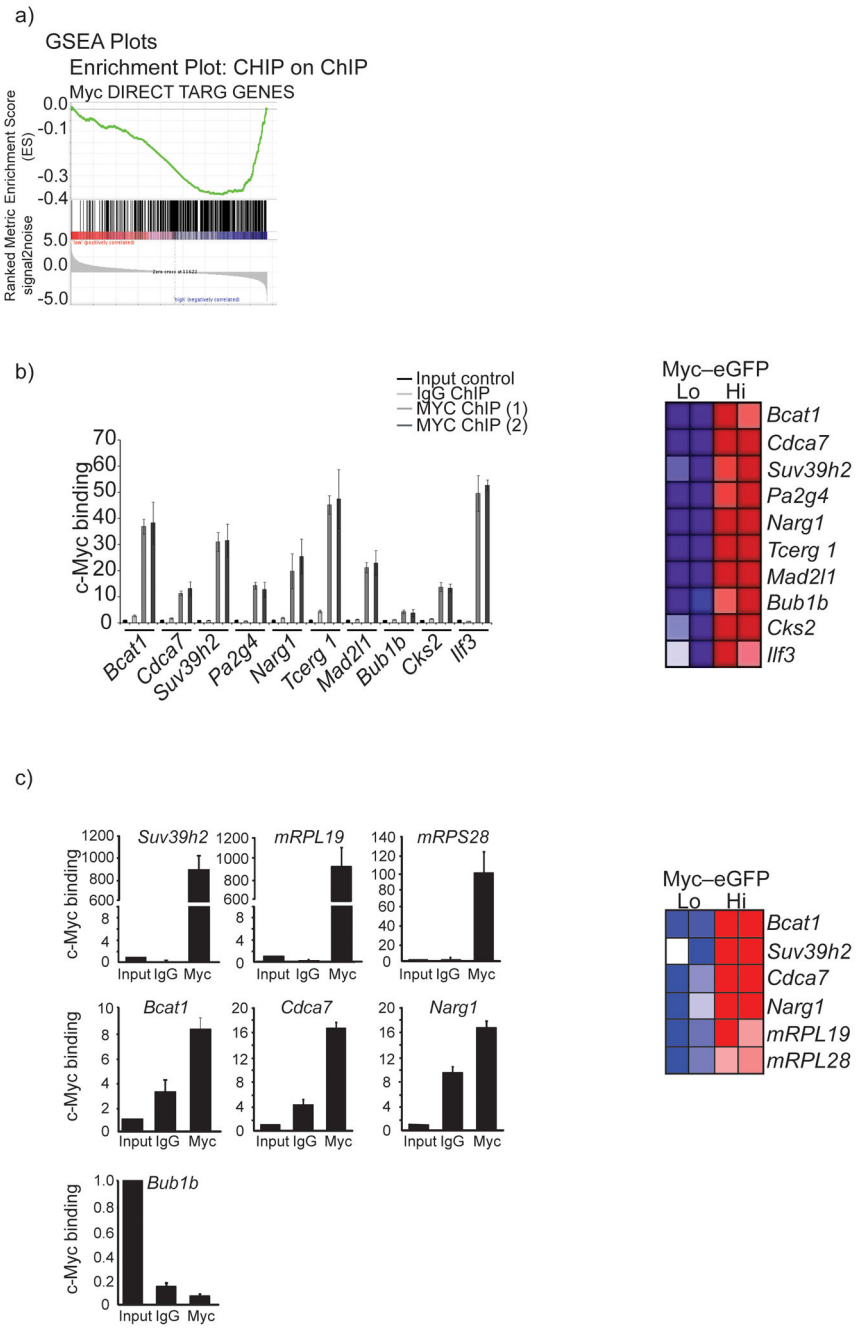

Figure 5. c-Myc protein abundance directly controls the molecular program of stem cell differentiation, cell cycle entry and self-renewal

a) Heat map demonstrating relative gene expression signatures of c-Myc-eGFP^{Hi} and c-Myc-eGFP^{Lo} subsets. A direct comparison to the relative gene expression in *Fbw7*$^{-/-}$ LSKs is also shown. **b)** Representative GSEA profiles showing positive correlation of the c-Myc-eGFP^{Lo} signature to stem cell gene sets and negative correlation to cell cycle and DNA replication gene sets. **c)** Representative GSEA profiles showing a positive correlation between both TGF-β and Wnt signaling pathways with c-Myc-eGFP^{Lo} gene expression data set.

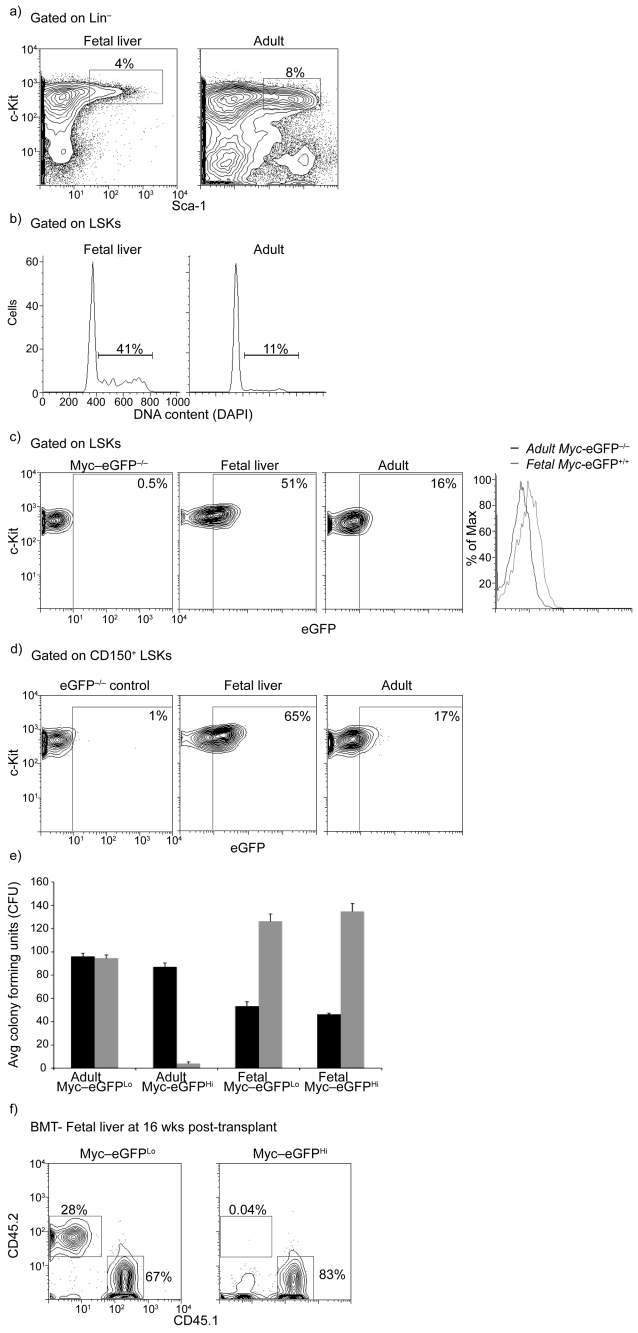

Figure 6. Genes over-expressed in c-Myc-EGFP^{Hi} cells are directly bound by the c-Myc transcription factor

a) GSEA analysis showing a positive correlation of c-Myc-eGFP^{Hi} gene expression profiles to a direct c-Myc target Chip-on-chip dataset. **b)** ChIP assay and Heat map of selected genes that are over-expressed in the c-Myc-eGFP^{Hi} cells. Red color: gene upregulation, Blue color: gene down-regulation. Two individual chromatin IPs using T-ALL cell line genomic DNA are shown. **c)** ChIP assay of selected genes using genomic DNA from purified Lineage^{-} c-Kit^{eGFP+} bone marrow progenitor cells. Also, Heat Map showing over

expression of selected genes in the c-Myc-eGFP^{Hi} LSK subset. Error bars indicate standard deviation (std) from 3 independent experiments.

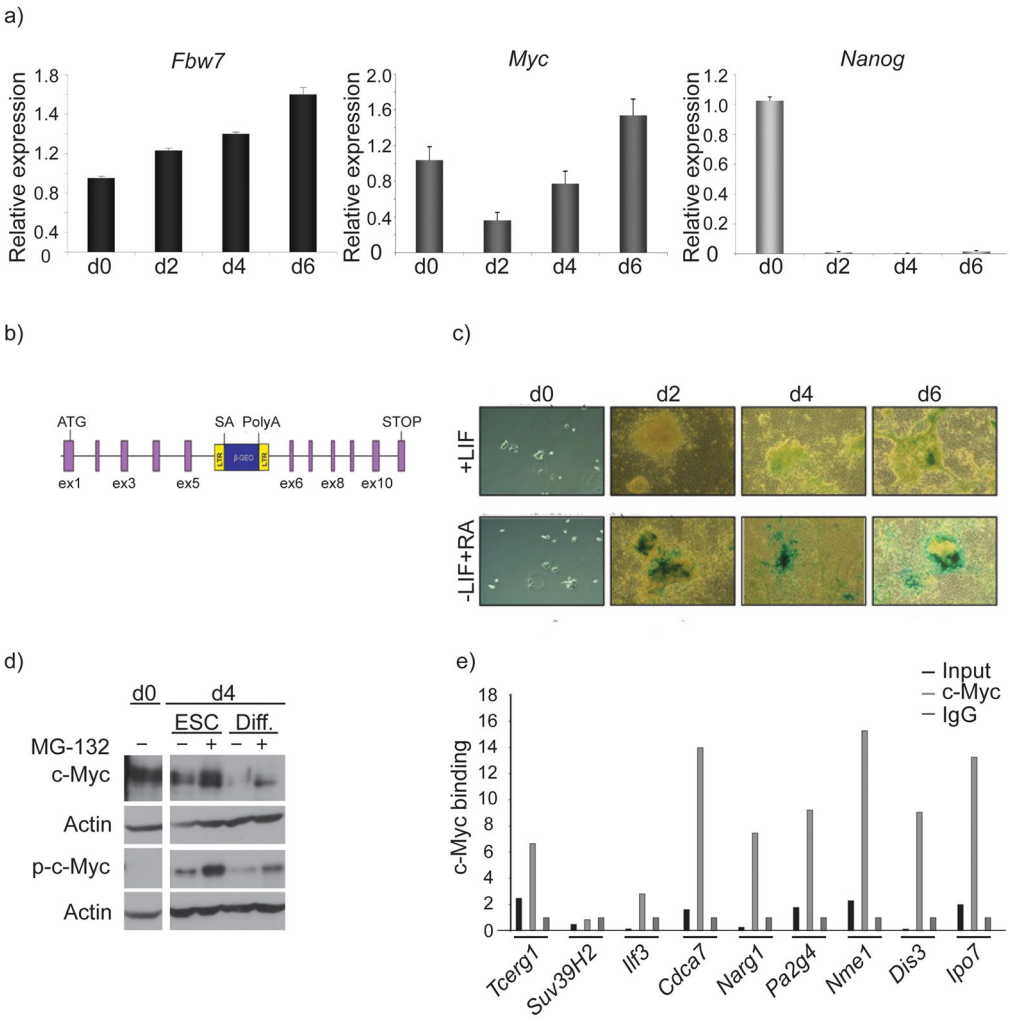

Figure 7. Patterns of Fbw7 and c-Myc expression in mouse embryonic stem cells

a) mRNA transcript expression levels of *Fbw7* (black), *Myc* (dark grey) and *Nanog* (light grey) in self-renewing (+LIF) and differentiating (−LIF, +RA) mouse ESC. Different days of differentiation (d0–6) are shown), **b)** Schematic diagram of *Fbw7* gene-trap cassette. **c)** LacZ staining in Murine ESCs containing the *Fbw7* gene trap cassette depicting upregulation of Fbw7 expression as Murine ESCs differentiate via the removal of LIF and the addition of Retinoic Acid (RA). **d)** Western blot showing stabilization of both phospho-(T58) and total-c-Myc in self-renewing and differentiating Murine ESCs treated with 20uM of proteosome inhibitor MG-132. **e)** ChIP assay was carried out using the specific regulators shown in Fig 6 revealing substantial enrichment upon c-Myc immunoprecipitation in Murine ESCs. Error bars indicate standard deviation (std) from 3 independent experiments.

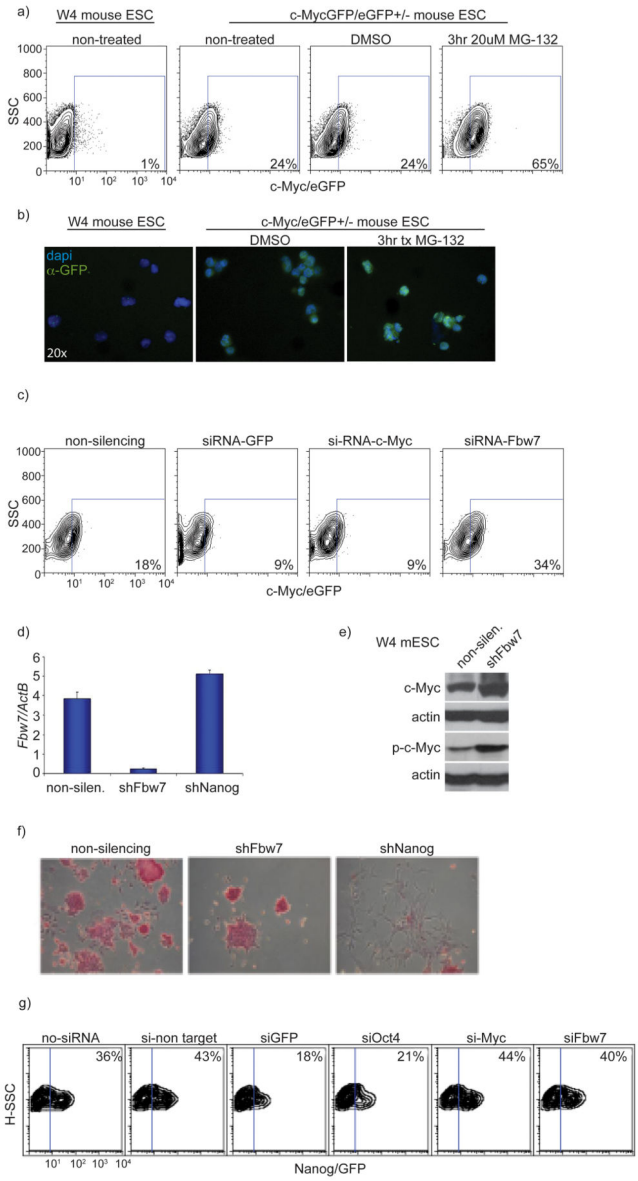

Figure 8. Fbw7 is dispensable for the self-renewal of Murine ESCs

a) Inhibition of proteasomal degradation via MG-132 treatment resulted in accumulation of c-Myc protein in *Myc*$^{eGFP/-}$ Murine ESCs. **b)** Visualization of c-Myc-eGFP in W4 and *Myc*$^{eGFP/-}$ Murine ESCs with and without treatment with MG-132. GFP (green), nuclear staining (DAPI) **c)** Knock-down of *Fbw7* using siRNA in *c-Myc*$^{eGFP/-}$ ESCs resulted in accumulation of c-Myc protein (increase in eGFP levels) while siRNA targeting both *Myc* and GFP showed a reduction in c-Myc-eGFP levels as assessed by FACs analysis. **d)** qRT-PCR of *Fbw7* mRNA expression in ESCs expressing shRNAs against *Fbw7* and *Nanog*. A non silencing shRNA is used as a control. **e)** Western blot depicting accumulation of both phospho (T58)-and total-c-Myc protein upon shRNA mediated knock down of *Fbw7* when compared to a non-silencing shRNA control. **f)** Alkaline phosphatase staining in Murine ESCs showed no difference in differentiation capacity upon shRNA mediated knock-down of *Fbw7* when compared to non-silencing control while silencing of *Nanog* resulted in

complete differentiation. **g)** siRNA knock-down of *Fbw7* in a *Nanog-eGFP* reporter ESC line resulted in no difference in Nanog-eGFP expression levels when compared to non-silencing control. Knock-down of *Oct4* resulted in a reduction of Nanog-eGFP expression levels (marking differentiation). Plots are a representation of at least 3 independent experiments